Insights into Soil NO Emissions and the Contribution to Surface Ozone Formation in China

Ling Huang[1,2], Jiong Fang[1,2], Jiaqiang Liao[1,2], Greg Yarwood[3], Hui Chen[1,2], Yangjun Wang[1,2], Li Li[1,2*]

[1]School of Environmental and Chemical Engineering, Shanghai University, Shanghai, 200444, China

[2]Key Laboratory of Organic Compound Pollution Control Engineering (MOE), Shanghai University, Shanghai, 200444, China

[3]Ramboll, Novato, California, 94945, USA

Correspondence: Li Li (lily@shu.edu.cn)

Keywords: Soil NO emissions; Ground-level ozone; BDSNP; OSAT

Abstract. Elevated ground-level ozone concentrations have emerged as a major environmental issue in China. Nitrogen oxide (NO_x) is a key precursor to ozone formation. Although control strategies aimed at reducing NO_x emissions from conventional combustion sources are widely recognized, soil NO_x emissions (mainly as NO) due to microbial processes have received little attention. The impact of soil NO emissions on ground-level ozone concentration is yet to be evaluated. This study estimated soil NO emissions in China using the Berkeley-Dalhousie soil NO_x parameterization (BDSNP) algorithm. A typical modeling approach was used to quantify the contribution of soil NO emissions to surface ozone concentration. The Brute-force method (BFM) and the Ozone Source Apportionment Technology (OSAT) implemented in the Comprehensive Air Quality Model with extensions (CAMx) were used. The total soil NO emissions in China for 2018 were estimated to be 1157.9 Gg N, with an uncertainty range of 715.7~1902.6 Gg N. Spatially, soil NO emissions are mainly concentrated in Central China, North China, Northeast China, northern Yangtze River Delta (YRD) and eastern Sichuan Basin, with distinct diurnal and monthly variations that are mainly affected by temperature and the timing of fertilizer application. Both the BFM and OSAT results indicate a substantial contribution of soil NO emissions to the maximum daily 8-hour (MDA8) ozone concentrations by 8~12.5 $\mu g/m^3$ on average for June 2018, with the OSAT results consistently higher than BFM. The results also showed that soil NO emissions led to a relative increase in ozone exceedance days by 10%~43.5% for selected regions. Reducing soil NO emissions resulted in a general decrease in monthly MDA8 ozone concentrations, and the magnitude of ozone reduction became more pronounced with increasing reductions. However, even with complete reductions in soil NO emissions, approximately 450.3 million people are still exposed to unhealthy ozone levels, necessitating

multiple control policies at the same time. This study highlights the importance of soil NO emissions for ground-level ozone concentrations and the potential of reducing NO emissions as a future control strategy for ozone mitigation in China.

1. Introduction

A substantial decrease in the atmospheric fine particulate matter ($PM_{2.5}$) concentrations has been witnessed during the past decade in China (Zhai et al., 2019; Xiao et al., 2020; Maji, 2020) while the ground-level ozone (O_3) concentrations do not exhibit a steady downward trend (Lu et al., 2020; Lu et al., 2021; Wang et al., 2022a; Sun et al., 2021). Because high ozone concentration increases respiratory and circulatory risks (Malley et al., 2017; Cakaj et al., 2023; Wang et al., 2020) and reduces crop yields (Feng et al., 2019; Lin et al., 2018; Mukherjee et al., 2021; Montes et al., 2022), the coordinate control of $PM_{2.5}$ and O_3 was proposed as part of the 14th Five-year plan (State Council, 2021). A continuous increase in summertime surface ozone was observed across China's nationwide monitoring network from 2013 to 2019, followed by an unprecedented decline in 2020 (except for Sichuan Basin) (Sun et al., 2021), which is equally attributed to meteorology and anthropogenic emissions reductions (Yin et al., 2021). As a secondary air pollutant, ozone is generated by the photochemical oxidation of volatile organic compounds (VOC) in the presence of nitrogen oxides ($NOx = NO + NO_2$), both of which are considered ozone precursors. The control strategies to mitigate ozone pollution in China focused on reducing NOx emissions at an early stage and started to stress the control of VOCs emissions in recent years (e.g., the 2020 action plan on VOCs mitigation), including control of fugitive emissions, stringent emissions standards, and substituting raw materials with low VOCs content (Ecology, 2020). Ding et al. (2021) concluded that for North China Plain (NCP), a region that experienced the most severe $PM_{2.5}$ and ozone pollution in China, reductions in NOx emissions are essential regardless of VOC reduction.

Existing control strategies for NOx emissions are almost exclusively targeted at combustion sources, for example, power plants, industrial boilers, cement production, and vehicle exhausts (Sun et al., 2018; Ding et al., 2017; Diao et al., 2018). However, NOx emissions from soils (mainly as NO), as a result of microbial processes (e.g., nitrification and denitrification), could make up a substantial fraction of the total NOx emissions (Lu et al., 2021; Drury et al., 2021), yet is often overlooked. In California, soil NOx emissions in July accounted for 40% of the state's total NOx emissions (when using an updated estimation algorithm) and resulted in 23% of enhanced surface ozone concentration (Sha et al., 2021). However, a wide range of annual soil NOx emissions from 8,685 tons (as NO_2, (Guo et al., 2020) to 161,100 metric tons of NOx-N (Almaraz et al., 2018) were reported depending on different methods. Romer et al. (2018) estimated that nearly half of the increase in hot-day

ozone concentration in a forested area of the rural southeastern United States is attributable to the temperature-induced increases in NOx emissions, mostly likely due to soil microbes.

Soil NO emissions are affected by many factors, including nitrogen fertilizer application, soil organic carbon content, soil temperature, humidity, and pH (Vinken et al., 2014; Yan et al., 2005; Wang et al., 2021; Skiba et al., 2021). The amount of nitrogen fertilizer application in China was estimated to account for one-third of the global nitrogen fertilizer application (Heffer and Prud'homme, 2016), with most of the land under high nitrogen deposition (Liu et al., 2013; Lü and Tian, 2007). Therefore, soil NO emissions in China are expected to be significant, and their impacts on ozone pollution need to be systematically evaluated. So far, only a limited number of studies have addressed this issue in China (Lu et al., 2021; Shen et al., 2023; Wang et al., 2008; Wang et al., 2022b). Lu et al. (2021) concluded that soil NO significantly reduced the ozone sensitivity to anthropogenic emissions in NCP, therefore, causing a so-called "emissions control penalty". Wang et al. (2022b) reported NOx emissions from cropland contributed 5.0% of the maximum daily 8h average ozone (MDA8 O$_3$) and 27.7% of NO$_2$ concentration in NCP. These studies focused solely on NCP, a region with persistent O$_3$ pollution in warm seasons (Liu et al., 2020; Lu et al., 2020). The impact of soil NO emissions on ozone concentrations over other regions, for example, the northern Yangtze River Delta (YRD) and Sichuan Basin, where soil emissions are high (see Section 3.1) and ozone pollution is also severe (Shen et al., 2022; Yang et al., 2021), has not been much evaluated in details (Shen et al., 2023). In addition, the method employed in existing studies to evaluate soil NO emissions on ozone concentration is the conventional "brute-force" zero-out approach, which might be inappropriate given the strong nonlinearity of the ozone chemistry (Clappier et al., 2017; Thunis et al., 2019).

With the deepening of emissions control measures for power, industrial and on-road sectors, anthropogenic NOx emissions from combustion sources have decreased at a much faster rate (by 4.9% since 2012) than that from soil (fertilizer application decreases at a rate of 1.5% since 2015, Fig. S1). Therefore, understanding the impacts of soil NO emissions on ground-level ozone concentration, particularly considering the spatial heterogeneities over different regions of China, is of great importance for formulating future ozone mitigation strategies. In this study, soil NO emissions in China for 2018 were estimated based on a most recent soil NO parameterization scheme with updated fertilizer data as input. The spatial and temporal variations of soil NO emissions were described first. Uncertainties associated with estimation of soil NO emissions were discussed. An integrated meteorology and air quality model was applied to quantify the impact of soil NO emissions on surface ozone concentration based on two different methods. Lastly, we evaluated the changes in ozone concentration and exposed population under different emission scenarios to highlight the effectiveness of reducing soil NO emissions as potential control policy. Our results provide insights into developing

111 effective emissions reduction strategies to mitigate the ozone pollution in China.

2. Methodology

2.1. Estimation of soil NO emissions in China

Soil NO emissions were estimated based on the Berkeley-Dalhousie Soil NOx Parameterization (BDSNP) that is implemented in the Model of Emissions of Gases and Aerosols from Nature (MEGAN) version 3.2 (https://bai.ess.uci.edu/megan/data-and-code, accessed on September 1st, 2021). The BDSNP algorithm estimates the soil NO emissions by adjusting a biome-specific NO emissions factor in response to various conditions, including the soil temperature, soil moisture, precipitation-induced pulsing, and a canopy reduction factor (Eq. 1, Rasool et al., 2016):

$$NO_{\text{emission flux}} = A'_{biome}(N_{avail}) \times f(T) \times g(\theta) \times P(l_{dry}) \times CRF(LAI, Biome, Meterology) \quad \text{Eq. 1}$$

where $f(T)$ and $g(\theta)$ is the temperature (T, unit: K) and soil moisture (θ, unit: m^3/m^3) dependence functions, respectively; $P(l_{dry})$ represents the pulsed soil emissions due to wetting of dry soils; l_{dry} (hours) is the antecedent dry period of a pulse; and CRF describes the canopy reduction factor, which is a function of the leaf area index (LAI, m^2/m^2) and the meteorology. A'_{biome} (ng N m^{-2} s^{-1}) is the biome-specific emission factor, which is further calculated as Eq.2:

$$A'_{biome} = A_{w,biome} + N_{avail} \times \bar{E} \quad \text{Eq. 2}$$

In Eq. 2, $A_{w,biome}$ (ng N m^{-2} s^{-1}) is the wet biome-dependent emission factor; N_{avail} is the available nitrogen from fertilizer and deposition; $\bar{E}$ is the emission rate based on an observed global estimates of fertilizer emissions (Rasool et al., 2016). The detailed expressions of these parameters are presented in the Supporting Information. More information on the BDSNP parameterizations can be found in previous studies (Hudman et al., 2012).

The default N fertilizer input data provided with the BDSNP algorithm is based on the a (Potter et al., 2010), which gives a number of 19.6 Tg N/a. In this study, we collected fertilizer data from statistical yearbooks at the provincial level. The total amount of pure nitrogen fertilizer (hereafter N fertilizer) applied in the year 2018 is 20.7 Tg N/a, which is similar (5.6% higher) to IFA value. However, besides the N fertilizer, NPK compound fertilizer (containing nitrogen (N), phosphorous (P), and potassium (K)) is being increasingly applied in China. According to the statistical yearbook, the amount of N fertilizer applied decreased from 23.5 Tg in 2010 to 20.7 Tg in 2018 (a relative reduction of 11.9%). In contrast, NPK fertilizer increased from 18.0 in 2010 to 22.7 Tg in 2018 (a relative increase of 26.1%). We assumed one-third of the NPK fertilizer is nitrogen (Liu, 2016); thus, the total amount of nitrogen applied as fertilizer is 28.2 Tg N in 2018, which is 43.9% higher than the value from Potter et al. (2010). We divided China into seven regions for emission analysis at regional

scale, namely Northeast China, North China, Central China, East China, South China, Southwest China, and Northwest China, as indicated by different colors in Fig. 1 (see Table S1 for the list of provinces in each region). At the regional level, the amount of total fertilizer differs by as much as 9.1% to 46.4% from the default fertilizer (Table S2).
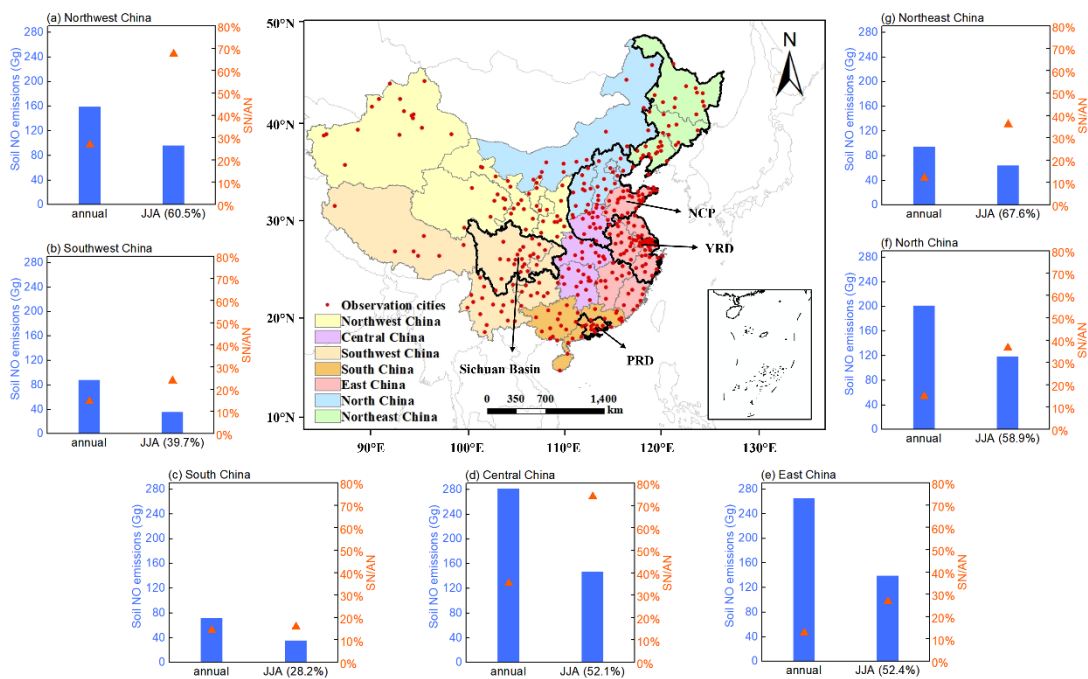
Figure 1. Modeling domain and region definitions. Surrounding charts show the annual and summer (June-July-August, JJA) soil NO emissions and ratio of soil NO to anthropogenic NOx emissions for each region.

2.2. Model configurations

A typical modeling approach was applied to evaluate the contribution of soil NO emissions to surface ozone concentration. The Weather Research and Forecasting (WRF) model (version 3.7, https://www.mmm.ucar.edu/wrf-model-general, accessed on December 1st, 2021) and the Comprehensive Air Quality Model with Extension (CAMx, version 7.0, http://www.camx.com/, accessed on December 1st, 2021) were applied to simulate the meteorological fields and subsequent ozone concentrations. Table S3 listed the detailed model configurations for WRF and CAMx. Anthropogenic emissions include the Multi-resolution Emission Inventory of China for 2017 (MEIC, http://www.meicmodel.org, accessed on December 1st, 2021) and the 2010 European Commission's Emissions Database for Global Atmospheric Research (EDGAR, http://edgar.jrc.ec.europa.eu/index.php, accessed on December 1st, 2021) for outside China. Biogenic emissions were calculated along with the soil NO emissions using MEGAN3.2. Open biomass burning emissions are adopted from the Fire INventory from NCAR version (FINN, version 1.5, https://www.acom.ucar.edu/Data/fire/) with MOZART speciation and converted to CAMx

CB05 model species. The gaseous and aerosol modules used in CAMx include the CB05 chemical mechanism (Yarwood et al., 2010) and the CF module. The aqueous-phase chemistry is based on the updated mechanism of the Regional Acid Deposition Model (RADM) (Chang et al., 1987). A base case simulation was conducted for June 2018 when soil NO emissions reached maxima (Section 3.1) and ozone pollution was severe over eastern China (Mao et al., 2020; Jiang et al., 2022). Base case model performances have been evaluated in our previous studies (Huang et al., 2021; Huang et al., 2022b). Here we evaluated simulated ozone concentrations using the Pearson correlation coefficient (R), mean bias (MB), root-mean-square error (RMSE), normalized mean bias (NMB), and normalized mean error (NME) against hourly observed ozone concentrations for 365 cities in China. The formula for each of the statistical metrics is given in Table S4. Observed hourly ozone concentrations were obtained from the China National Environmental Monitoring Center.

2.3. Brute-force and OSAT

In this study, two methods were used to quantify the impact of soil NO emissions on surface ozone concentration during the simulation period. The first is the conventional brute-force method (BFM), which involves comparing the simulated ozone concentration between the base case and a scenario case without soil NO emissions. The difference between these two scenarios was considered to represent the contribution of soil NO emissions to ozone. The second method applies the widely used Ozone Source Apportionment Technology (OSAT) implemented in CAMx (Yarwood et al., 1996), with soil NO emissions being tagged as an individual emission group. OSAT attributes ozone formation to NO_x or VOCs based on their relative availability and apportions NO_x and VOCs emissions by source group/region (Ramboll, 2021). In addition to soil NO emissions, anthropogenic and natural emissions (including biogenic VOC emissions, lightning NO emissions, and open biomass burning) were also tagged as individual emission groups.

3. Results and discussions

3.1. Soil NO emissions for 2018 in China

3.1.1. Spatial and temporal variations

National total soil NO emissions for 2018 is estimated to be 1157.9 Gg N, with an uncertainty range of 715.7~1902.6 Gg N, which will be discussed more in Section 3.1.2. On an annual scale, soil NO emissions accounted for 17.3% of the total anthropogenic NO_x emissions in China for 2017 (based on MEIC inventory). This ratio varies from 12.0% to 35.3% at regional scale. Unlike the anthropogenic NO_x emissions that concentrate over densely populated regions (e.g., NCP, YRD), soil NO emissions are most abundant in Central China, particularly Henan Province and nearby provinces, including Hebei and Shandong in the NCP, Jiangsu

201 and Anhui in northern YRD (Fig. 2a). Other hotspots of soil NO emissions include Northeast
202 China and the eastern part of the Sichuan Bain. As expected, the spatial distribution of soil
203 NO emissions closely mirrors that of the fertilizer application (Fig. 2b). Henan (located in
204 Central China), Shandong (NCP), and Hebei (NCP) are the top three provinces that have the
205 highest fertilizer application (together accounting for 24.1% of national totals in 2018) and
206 thus highest soil NO emissions (together accounting for 35.7%).
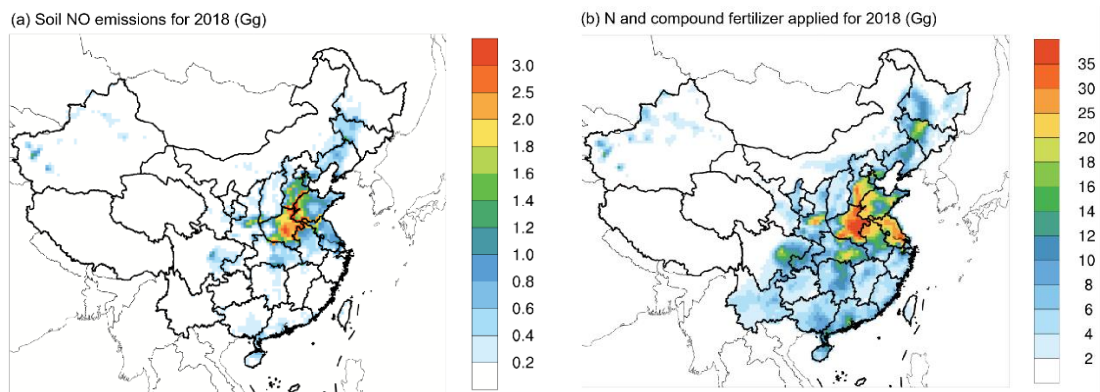
207 **Figure 2.** Spatial distribution of (a) soil NO emissions for 2018 and (b) N and compound
208 fertilizer applied for 2018.

209 In terms of the monthly variations, the total soil NO emissions show a unimodal pattern (as
210 shown in Fig. 3a with the highest emissions occurring in the summer months of June, July,
211 and August), except for South China and Southeast China (Fig. S2), where the peak emissions
212 occur in April or May. Soil NO emissions during the summer months account for 28.2%
213 (South China) to 67.6% (Northeast China) of the annual totals (Fig. 1 and Table S5). The
214 shape of monthly soil NO emissions is influenced by temperature and the timing of fertilizer
215 application. The BDSNP algorithm assumes that 75% of the annual fertilizer is applied over
216 the first month of the growing season, with the remaining 25% applied evenly throughout the
217 rest of the growing season. This assumption results in a significant amount of fertilizer being
218 applied from April to August (Fig. 3a). In contrast, anthropogenic NOx emissions display
219 weaker monthly variations (Zheng et al., 2021). Consequently, the ratio of soil NO emissions
220 to anthropogenic NOx (SN/AN) is much higher during the summer months. In regions such as
221 Central China and Northwest China, where soil NO emissions are high and anthropogenic
222 NOx emissions are relatively low, SN/AN reaches 74.0% and 67.5% during the summer
223 months (Fig. 1 and Table S5). In East China and North China, where anthropogenic NOx
224 emissions are high, SN/AN ranges from 26.8% to 36.5% during the summer months. These
225 findings are align with Chen et al. (2022), who reported that soil NO emissions made up 28%
226 of total NOx (soil NO + anthropogenic NOx) emissions in summer and could reach 50–90%
227 in isolated areas and suburbs. The substantial contribution of soil NO emissions during the
228 ozone pollution season implies a potentially significant impact on surface ozone

concentration. In terms of diurnal variations, soil NO emissions peak in the afternoon due to diurnal temperature fluctuations. As illustrated by Fig. 3b, the average hourly soil NO emissions over NCP for June 2018 closely follow the WRF simulated temperature changes. The BDSNP algorithm identifies three sources of soil nitrogen: background, atmospheric nitrogen deposition, and fertilizer application, with the latter being the primary contributor. A decomposition analysis of soil NO emissions for NCP reveals that fertilizer application accounts for 83.4% of total NO soil emissions (Fig. 3b), while background and atmospheric nitrogen deposition only contribute for 11.2% and 5.4%, respectively. Thus, although soil NO emissions are generally considered a "natural" source (Galbally et al., 2008) and are not currently targeted in NOx emission mitigation strategies, human fertilizer activities render soil NO emissions an anthropogenic source.
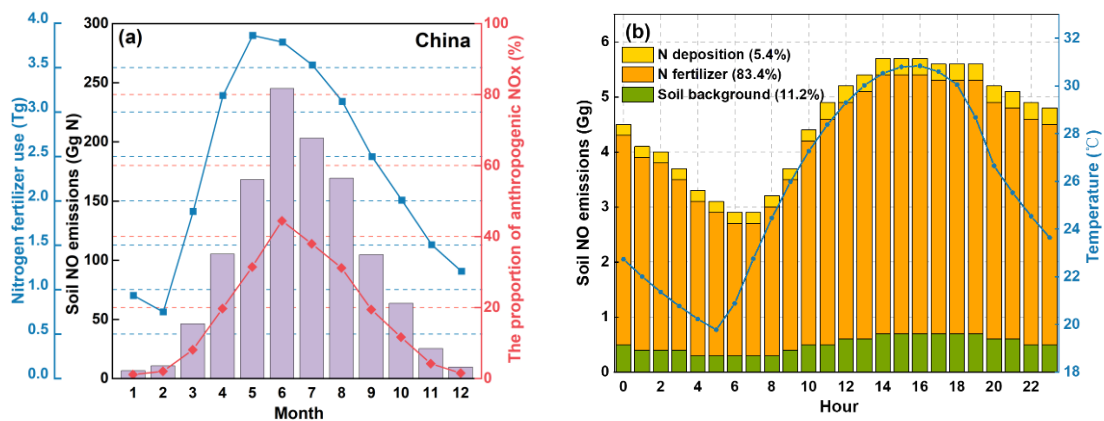
Figure 3. (a) Monthly fertilizer (N + compound) applied and soil NO emissions in China and (b) hourly soil NO emissions for 2018 June in NCP and domain-averaged hourly 2-m temperature simulated by WRF.

3.1.2. Limitations and Uncertainties associated with soil NO emission estimation

Although the current BDSNP algorithm is considered more sophisticated than the old YL95 algorithm, it still suffers certain limitations. For example, the current BDSNP parameterization employs a static classification of "arid" versus "non-arid" soils, upon which the relationship between soil NO emissions and soil moisture relies (Hudman et al., 2012). However, recent studies (Sha et al., 2021; Huber et al., 2023) have shown more dynamic representation of this classification is needed to capture the emission characteristics as observed by many chamber and atmospheric studies (e.g., Oikawa et al. 2015; Huang et al. 2022a). Huber et al. (2023) also showed that the emission estimated based on the static classification are very sensitive to the soil moisture and thus could not produce self-consistent results when using different soil moisture products.

In addition to the aforementioned limitation, the estimated soil NO emissions are also subjected to certain limitations and large uncertainties. The first uncertainty comes from the

amount of fertilizer application, which has been identified as the dominant contributor to soil NO emissions, as mentioned above. According to the global dataset (Potter et al., 2010), the amount of fertilizer applied is 19.6 Tg, which is comparable to the sum of nitrogen fertilizer for 2018 (20.7 Tg) obtained from provincial statistical yearbooks. However, compound fertilizer, usually with a nitrogen, phosphorus, and potassium ratio of 15: 15: 15, has been used more in China. Since 2016, the amount of nitrogen fertilizer has been decreasing annually at an average rate of 4.6%, while the amount of compound fertilizer has been increasing since 2010 at an average rate of 3.3%. The ratio of compound fertilizer to nitrogen fertilizer has increased from 76.4% in 2010 to 109.8% in 2018. Consequently, soil NO emissions may be largely underestimated if the compound fertilizer is not taken into account. Our calculation shows that if only nitrogen fertilizer is considered, the estimated total soil NO emissions are 805.2 Gg N/a for 2018, which is comparable to the value (770 Gg N/a averaged during 2008-2017) reported by Lu et al. (2021), but 30.5% lower than that based on both nitrogen fertilizer and compound fertilizer. Regionally, this underestimation ranges from 11.1%~41.5%, with a larger underestimation in Central China and East China (Fig. S3).

Another major uncertainty in estimating soil NO emissions is the temperature dependence factor $f(T)$ in Eq.1. According to the BDSNP scheme, soil NO emissions increase exponentially with temperature between 0 and 30°C and reach a maximum when the temperature exceeds 30°C. The default temperature dependence coefficient (i.e., k in Eq. S2) follows the value used in the YL95 scheme, which is 0.103±0.04. However, as shown by Table 3 in Yienger and Levy (1995), this value is the weighted average of values reported for different land types, which shows a wide range from 0.040 to 0.189. Even for the same crop type (e.g., corn), the value of k could be quite different (0.130 vs. 0.066). We conducted a sensitivity analysis to examine the impact of varying the k value on estimated soil NO emissions. When the k value decreases or increases by 20%, the estimated total soil NO emissions change from 715.7 to 1902.6 Gg N/a, representing a relative difference of -38.2~64.3% deviation from the default value (1157.9 Gg N/a). Using the default k value would result in a large overestimation of simulated NO_2 concentrations over NCP and YRD and underestimation over Northeast China (Fig. S4). According to the total sown areas of farm crops reported in the provincial statistical yearbook, the primary crops grown in these regions are wheat and corn, which have a relatively low k value (0.066~0.073). Therefore, we adjusted k for NCP (reduced by 20%), YRD (reduced by 10%), and Northeast China (increased by 10%). CAMx simulation results show that this adjustment would not significantly affect the simulated MDA8 O_3 concentration but could reduce the NO_2 gap between observation and simulation (Fig. S4-S5). Therefore, we applied this adjustment to soil NO emissions in the following CAMx simulations.

292   3.2. Contribution of soil NO emissions to ground-level ozone

293   3.2.1. Base case model evaluation

294   Fig. 4 shows the monthly averaged MDA8 ozone concentration simulated for June 2018 with

295   observed values presented on top. Overall the model well captured the spatial distribution of

296   MDA8 with a spatial correlation R = 0.89. Over the 365 cities in China, the simulated

297   monthly averaged MDA8 ozone concentration is 146.7±36.1 μg/m^3, which is slightly higher

298   than the observed value of 129.6±37.6 μg/m^3 (NMB = 13.2%). Regionally, model shows

299   better performance in Northeast China (MB = 2.4 μg/m^3, NMB = 1.9%) and NCP (MB = 13.3

300   μg/m^3, NMB = 7.7%). Over-prediction is observed for Sichuan Basin and YRD (Table S6).

301   Simulated ozone concentration over the northwest Qinghai-Tibet Plateau was also much

302   higher than observed values. Our OSAT results (shown later) show that the high ozone

303   concentration over the Qinghai-Tibet Plateau is mostly contributed by the transport of

304   boundary ozone, which includes both horizontal and vertical (i.e., stratosphere) directions. For

305   regions with high altitude (e.g., the Qinghai-Tibet Plateau), vertical ozone intrusion from the

306   stratosphere is most substantial, which is consistent with the finding by Chen et al. (2023) that

307   the boundary layer height was identified as the most important feature for ozone over the

308   Qinghai-Tibet Plateau.
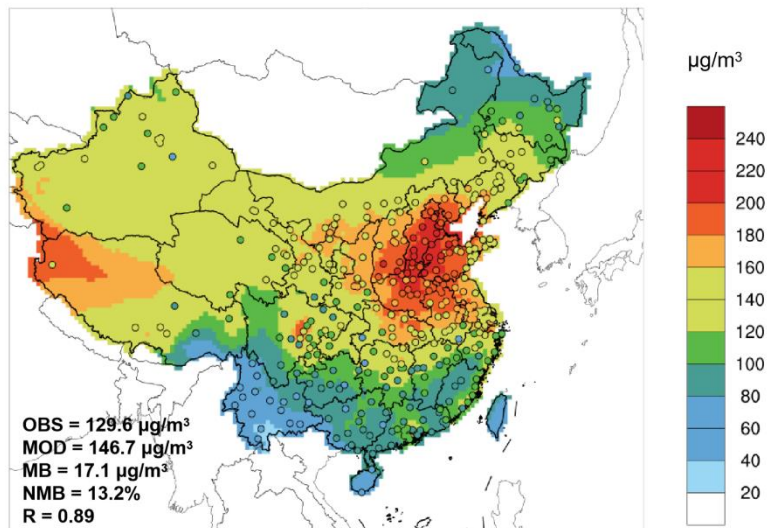
309

310   **Figure 4.** Comparison of simulated (base colors) and observed (scatter points) values of

311   MDA8 ozone in China in June 2018.

312   3.2.2. Impacts on regional ozone

313   To assess the contribution of soil NO emissions to surface ozone, both the brute-force method

314   (BFM) and the OSAT method were applied, and the results are shown in Fig. 5. Generally, the

315   two methods show consistent ozone contribution from soil NO emissions but with different

316   magnitudes. The BFM method shows widespread ozone enhancement due to soil NO

emissions with a spatial pattern that aligns with the distribution of soil NO emissions. Substantial ozone enhancement is found over Central China, Sichuan Basin, northern YRD, and eastern Northeast China. Maximum ozone enhancement (ΔMDA8) due to soil NO emissions is 26.4 $\mu g/m^3$ with a domain-average value of 8.0 $\mu g/m^3$. For selected key regions, the ozone contribution ranges from low to high: PRD (3.8$\pm$1.1 $\mu g/m^3$), YRD (8.7$\pm$4.7 $\mu g/m^3$), Sichuan Basin (9.1$\pm$0.9 $\mu g/m^3$), Northeast (9.3$\pm$3.0 $\mu g/m^3$), and NCP (13.9$\pm$4.4 $\mu g/m^3$), respectively. A similar spatial pattern is observed with the OSAT results, but the magnitudes are much higher. Maximum ozone contribution by soil NO emissions reaches 40.4 $\mu g/m^3$ according to OSAT results, which is 53.0% higher than the brute force method. The corresponding ozone contribution for each selected region is 6.7$\pm$1.2 $\mu g/m^3$ (PRD), 13.5 $\pm$7.4 $\mu g/m^3$ (Sichuan Basin), 14.5$\pm$4.9 $\mu g/m^3$ (Northeast China), 16.2$\pm$7.8 $\mu g/m^3$ (YRD) and 25.7$\pm$5.3 $\mu g/m^3$ (NCP). The scatter plots between BFM and OSAT results show good correlations (Fig. S6, R^2 = 0.78~0.97), with OSAT results higher by 10%~61%. For YRD, Sichuan Basin, and Northeast, the difference between the OSAT method and BFM increases with the absolute ozone concentration (Fig. S7), while NCP shows the opposite trend. The difference between the two methods reflects the nonlinear ozone response to NOx emissions. This nonlinearity becomes stronger in regions with larger NOx concentrations, especially where O_3 production is characterized as NOx-saturated (or VOC-limited), such as the NCP. In such cases, removing a portion of the NO emissions (e.g., zeroing out soil NO for the BFM simulation) makes O_3 production from the remaining NO emissions more efficient, which lessens the O_3 response. As shown later in Figure 7a, the O_3 response for NCP is more curved (nonlinear) than other regions, consistent with NCP tending to have more NOx-saturated O_3 production. This nonlinear effect also explains smaller O_3 attribution to soil NO by the BFM than OSAT, especially over the NCP. Attributing a secondary pollutant to a primary emission (e.g., O_3 to NO) is inherently tricky with nonlinear chemistry, as Koo et al. (2009) discussed. Therefore, it is useful to present estimates from different methods. The Path Integral Method (PIM) is a source apportionment method that explicitly treats nonlinear responses with mathematical rigor (Dunker et al., 2015). However, applying the PIM is more costly than the BFM or OSAT.

In addition to soil NO contribution, OSAT also gives ozone contributions from other source groups, including anthropogenic emissions within China, boundary contribution, natural emissions (e.g., biogenic emissions, open biomass burning, lightning NOx), and emissions outside China. The spatial distribution for each source category is presented in Fig. S8, and the relative contribution for each selected region is shown in Fig. S9. Overall, boundary transport (56.5%) and anthropogenic emissions (24.0%) contribute most to MDA8 ozone for June 2018. Boundary contribution is high over the western and northern parts of China, while the contribution from anthropogenic emissions is substantial over eastern China, where

354 anthropogenic emissions are extensive. On a national scale, soil NO emissions exhibit a
355 relative ozone contribution of 9.1%, and regionally this value ranges from 6.1% in PRD to
356 13.8% in NCP.
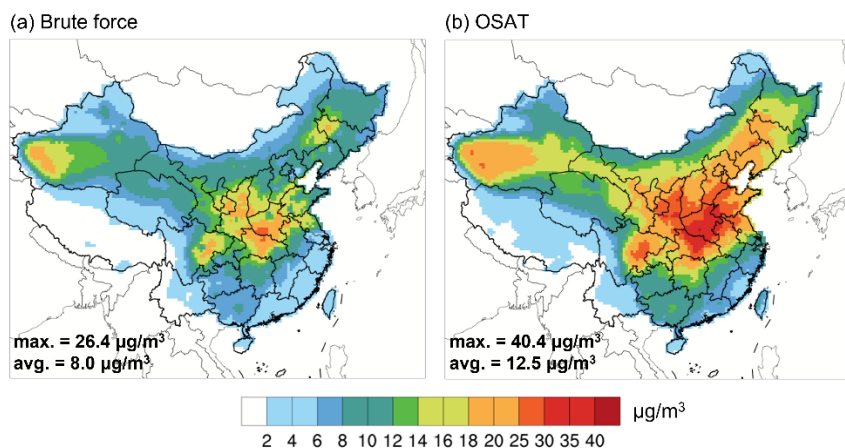
357
358 **Figure 5.** Ozone contribution from soil NO emissions based on (a) brute force method and (b)
359 OSAT method.

360 We further evaluated the impact of soil NO emissions on the number of ozone exceedances
361 days (i.e., days with MDA8 O_3 higher than 160 μg/m^3) during June 2018 based on the relative
362 response factor (RRF) method and results from the brute force method. The total number of
363 ozone exceedances days during June 2018 for the five selected regions ranged from 50 days
364 in PRD to 985 days in NCP (Table 1). The number of ozone exceedance days per city ranged
365 from 3.1 days in Sichuan Basin to 18.2 days in NCP, suggesting the severe ozone pollution in
366 June 2018 over NCP. RRF was first calculated for each city as the ratio of simulated ozone
367 concentration between the base case and the case with soil NO emissions excluded and
368 applied to the observed ozone concentrations to obtain adjusted ozone concentrations without
369 soil NO emissions. Soil NO emissions are estimated to lead to 121 ozone exceedance days in
370 NCP, followed by 84 days in the Northeast and 70 days in YRD, corresponding to a percent
371 change of 12.3%, 32.8%, and 10.5%, respectively. In Sichuan Basin, where soil NO emissions
372 are also substantial, soil NO emissions contribute 30 ozone exceedances days, which accounts
373 for 43.5% of the total ozone exceedances days. These results suggest the substantial
374 contribution of soil NO emissions to the number of ozone pollution days over regions with
375 high soil NO emissions.

376 **Table 1.** Number of ozone exceedances over selected regions during June 2018.

Region (No. of cities)	Number of ozone exceedance days (% of total days)	Δozone exceedances days when soil NO emissions are removed	% of total ozone exceedances days
NCP (54)	985 (60.8%)	-121	-12.3%
YRD (55)	666 (41.1%)	-70	-10.5%

PRD (9)	50 (18.5%)	-6	-12.0%
Sichuan Basin (22)	69 (10.5%)	-30	-43.5%
Northeast (37)	256 (23.1%)	-84	-32.8%

377 3.3. Ozone responses to reductions in soil NO emissions

378 Current NOx emission control policies primarily target combustion sources, such as power

379 plants (Du et al., 2021) and on-road vehicles (Park et al., 2021). Nitrification inhibitors, such

380 as dicyandiamide (DCD, $C_2H_4N_4$), have been found to be effective in reducing nitrogen loss,

381 thereby reducing NO emissions from soil (Abalos et al., 2014). Studies have shown that using

382 5% DCD with nitrogen fertilizer can reduce NO emissions by up to 70% (Xue et al., 2022). In

383 light of this, it is important to evaluate the impact of reduced soil NO emissions on ozone

384 concentration. To address this question, four sensitivity simulations were carried out for June

385 2018, with soil NO emissions reduced by 25%, 50%, 75%, and 100% relative to the base

386 case. As shown by Fig. 6, reducing soil NO emissions led to a general decrease in monthly

387 MDA8 ozone concentration (ΔMDA8), with the magnitude of ΔMDA8 becoming more

388 significant with the reduction ratio. With a 25% reduction in soil NO emissions, there was a

389 widespread small decrease in monthly average MDA8 ozone concentration (ΔMDA8: -

390 1.5±0.9 $\mu g/m^3$), except over NCP where ozone showed a slight increase (up to 1.3 $\mu g/m^3$) in

391 Shandong and Henan province. When soil NO emissions were cut by 50%, ΔMDA8 showed a

392 ubiquitous decrease across entire China with an average ΔMDA8 of -5.5 $\mu g/m^3$. When soil

393 NO emissions were removed entirely, the maximum ΔMDA8 could exceed 25 $\mu g/m^3$ over

394 central China, part of the Sichuan Basin, Northeast China, and Northeast China. Regions with

395 strong ozone responses generally aligned with regions that also had high soil NO emissions.

396 However, it should be noted that the ozone response to soil NO reductions not only depends

397 on the magnitude of soil NO emissions but is also affected by (1) the local ozone formation

398 regime that is further determined by the relative abundance of NOx and VOCs, and (2)

399 changes in transport of upwind ozone.
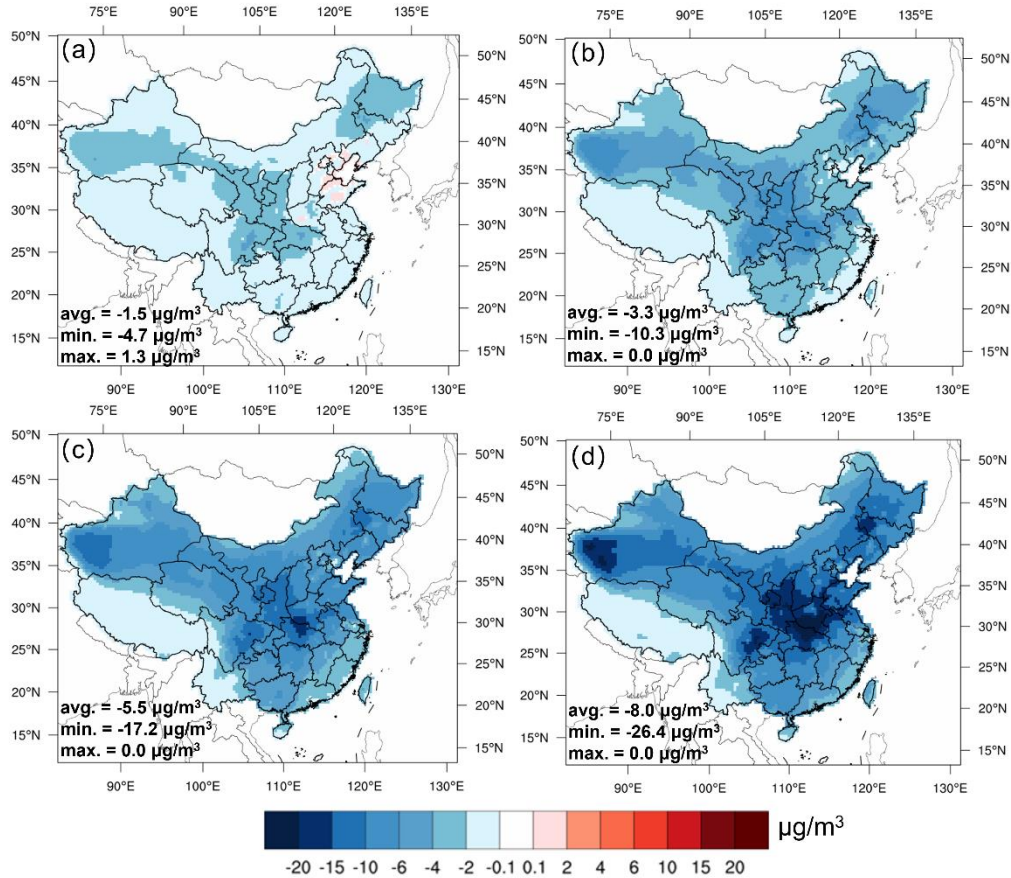
Figure 6. Spatial distribution of ΔMDA8 under (a) 25%, (b) 50%, (c) 75%, and (d) 100% reductions of soil NO emissions in June 2018.

Fig. 7a provides further details on the domain-averaged ΔMDA8 under different reduction scenarios for the five key regions. As expected, the ozone response in each region increased as the reduction in the soil NO emissions increased. NCP exhibited the strongest ozone responses to changes in soil NO emissions, with ΔMDA8 increasing from -0.7±0.8 μg/m^3 with 25% reductions to -13.9±4.4 μg/m^3 when all soil NO emissions were removed. YRD, Sichuan Basin, and Northeast China exhibit similar ozone responses when soil NO emissions are reduced. Under the 25% scenario, ΔMDA8 ranged from -4.7 to 1.3 μg/m^3 for these three regions; with 100% soil NO reductions, ΔMDA8 ranged from -21.4 to -0.9 μg/m^3. ΔMDA8 in PRD was relatively small. Even with a 100% reduction, the average ΔMDA8 in PRD was less than 5 μg/m^3, which is associated with the small soil NO emissions in PRD. It is interesting to note that all regions except NCP exhibited an approximate linear ozone response to changes in soil NO emission reductions. NCP showed more significant ozone reductions as the reduction ratio increased, suggesting that NCP would gain more benefits with more aggressive reductions in soil NO emissions compared to other regions.
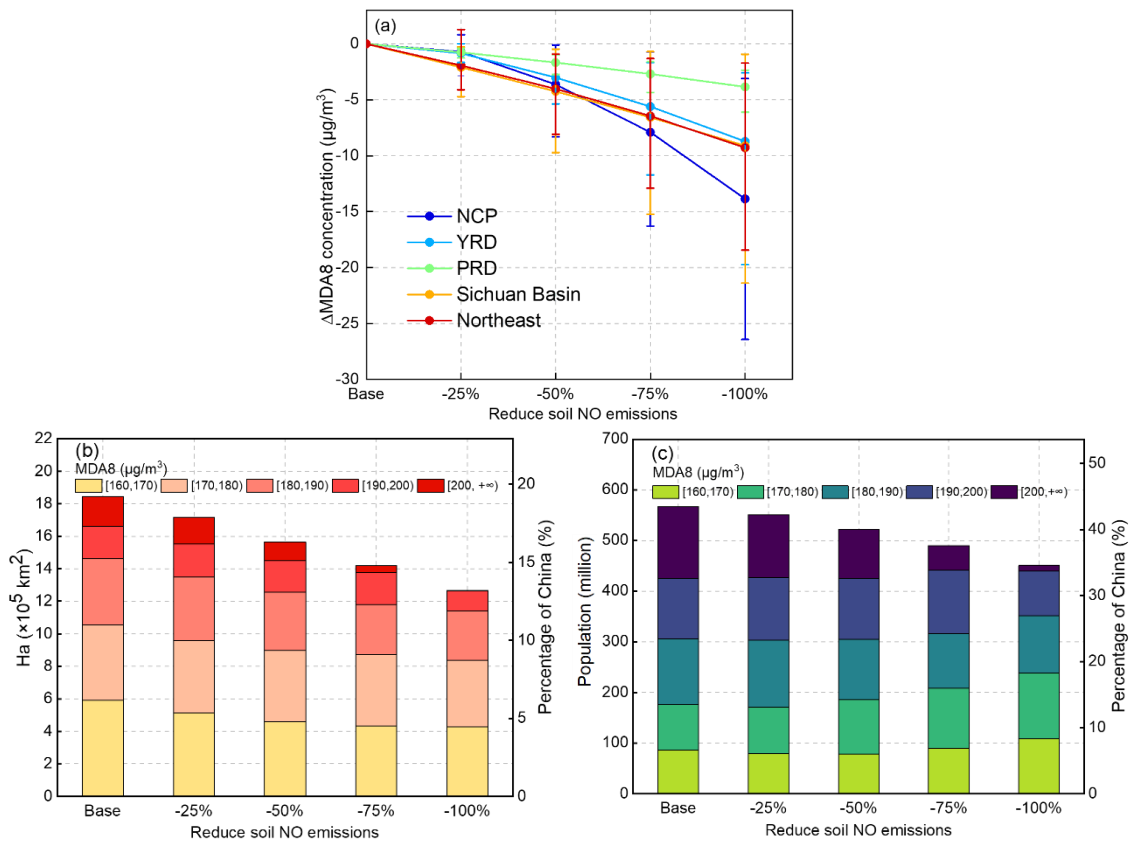
Figure 7. (a) ΔMDA8 concentrations in five key regions under different emission reduction scenarios (b) Area and (c) population exposed to different ozone levels under different soil NO emission reduction scenarios.

We evaluated the impact of different soil NO emission reduction scenarios on the area and population exposed to varying ozone levels. The results, presented in Fig. 7b and 7c, revealed a decrease in coverage and exposed population under high ozone concentrations as soil NO emissions decrease. The data presented in the plots are for grid cells with monthly MDA8 ozone concentrations exceeding 160 μg/m³. In the Base scenario, the estimated coverage of MDA8 ozone exceeding 160 μg/m³ was 1.84×10^6 km², equivalent to 19.2% of the national land area. The population exposed to ozone concentrations exceeding 160 μg/m³ amounts to 566.6 million, representing 43.4% of the entire population. The areas with extremely high ozone concentrations (MDA8 > 200 μg/m³) account for 1.9% of the national land area, with a corresponding exposed population of 10.9%, indicating that densely populated areas experience higher ozone concentrations. When soil NO emissions are halved, there is a 15.2% reduction in the coverage of non-attainment areas and an 8.0% reduction in the total exposed population. If soil NO emissions are eliminated, the total area coverage and population exposed to MDA8 ozone concentrations exceeding 160 μg/m³ would be 1.27×10^6 km² and 450.3 million, respectively, representing 13.2% and 34.5% of the total. Compared to the Base scenario, a 100% theoretical reduction in soil NO emissions leads to a 31.3% and 20.5%

reduction in the exposed area and population under high ozone concentration, respectively, indicating substantial health benefits gained when soil NO emissions are mitigated.

Fig. S10-S11 displays similar area and population plots for selected key regions. The overall trends for each sub-region are consistent. With 100% reductions in soil NO emissions, the area with high ozone concentration decreased by 17.8%, 22.3%, 65.4%, and 100% for NCP, YRD, Sichuan Basin, and Northeast. The corresponding values for the exposed population are 91.4%, 60.3%, 9.8%, and 0.0%. While the relative change is more significant in Sichuan Basin and Northeast China, NCP and YRD gain more health benefits due to the significantly higher total population for these two regions. However, it is worth noting that even with the complete elimination of soil NO emissions, a total of 450.3 million people are still exposed to ozone levels exceeding the national standard, necessitating multiple control policies at the same time, such as synergistic control of anthropogenic VOC emissions (Chen et al., 2022; Ding et al., 2021).

3.4 Comparison with existing studies

The soil NO emissions estimated in this study were also compared with values reported by existing studies based on either field measurement or model estimation (Table S7). Previous studies report a wide range of soil NO emissions from 480 to 1375 Gg N and soil NO flux ranging from 10 to 47.5 ng N m^{-2} s^{-1}. The soil NO emissions estimated in our study are 1157.9 Gg N with the default k value and 951.9 Gg N with region-adjusted k value, which falls within the upper range of previously reported values. The averaged soil NO flux over NCP in June 2018 estimated in our study is 35.4 ng N m^{-2} s^{-1}, which is within the range reported by previous studies (12.9~40.0 ng N m^{-2} s^{-1}).

The simulated ozone contribution by soil NO emissions is compared with other studies. In California, soil NO was estimated to cause a 23.0% increase in surface O_3 concentrations (Sha et al., 2021). Constrained by satellite measured NO_2 column densities, Wang et al. (2022b) reported MDA8 ozone contribution of 9.0 $\mu g/m^3$ (relative contribution of 5.4%) from cropland NOx emissions over NCP during a growing season in 2020. Lu et al. (2021) showed an interactional effect of domestic anthropogenic emissions with soil NO emissions of 9.5 ppb in the NCP during July 2017. In addition, soil NOx emissions strongly affect the sensitivity of ozone concentrations to anthropogenic sources in the NCP. In a most recent study by Shen et al. (2023), addition of the soil NOx emissions was shown to result in up to 15 ppb increase of ozone concentration over Xinjiang, Tibet, Inner Mongolia, and Heilongjiang, although a minor reduction was evident over the Yangtze River basin. When soil NOx emissions were reduced by 30%, ozone concentrations increased by 3-5 ppb over Inner Mongolia, Heilongjiang, Xinjiang, and Tibet, while decreased by 0-2 ppb over the Yangtze River basin. Surprisingly, when soil NOx emissions were increased by 30%, nearly identical ozone

responses were observed.

4. Conclusions

Soil NO emissions are non-negligible NOx sources, particularly during summer. The importance of soil NO emissions to ground-level ozone concentration in China is much less evaluated than combustion NOx emissions. In this study, the total national soil NO emissions were estimated to be 1157.9 Gg N in 2018, with a spatial distribution closely following that of fertilizer application. High soil NO emissions were mainly concentrated over Henan, Shandong, and Hebei provinces, which differs from anthropogenic NOx emissions. Distinct diurnal and seasonal variations in soil NO emissions were simulated, mainly driven by the changes in temperature as well as the timing of fertilizer application. Uncertainty analysis reveals a range of 715.7~1902.6 Gg N of soil NO emissions that warrant further constraints from observations.

Using two methods (BFM and OSAT), we evaluated the contribution of soil NO emissions to ground-level ozone concentration for June 2018. Both methods suggest a substantial contribution of soil NO emissions to MDA8 ozone concentrations by 8~12.5 µg/m^3 on average for June 2018, with the OSAT results consistently higher than BFM. Soil NO emissions were shown to lead to a relative increase of ozone exceedances days by 10.0%~43.5% for selected regions. Reducing soil NO emissions could generally reduce the ground-level ozone concentrations and populations exposed to unhealthy ozone levels (MDA8 > 160 µg/m^3), especially over NCP and YRD. With a 50% reduction in soil NO emissions, the coverage of non-attainment areas and the population exposed to unhealthy ozone levels decreased by 15.2% and 8.0%, respectively. However, even with the complete removal of soil NO emissions, approximately 450.3 million populations are still exposed to unhealthy ozone levels, necessitating multiple control policies at the same time, such as synergistic control of anthropogenic VOC emissions.

Data availability. Data will be made available on request.

Author contributions. Ling Huang: Conceptualization, Formal analysis, Writing – original draft. **Jiong Fang:** Data curation, Formal analysis, Visualization. **Jiaqiang Liao:** Data curation, Formal analysis, Visualization. **Greg Yarwood:** Writing – review & editing. **Hui Chen:** Writing – review & editing. **Yangjun Wang:** Writing – review & editing. **Li Li:** Conceptualization, Supervision, Funding acquisition, Writing – review & editing.

Competing interests. The authors declare that they have no known competing financial interests or personal relationships that could have appeared to influence the work reported in this paper.

Acknowledgments. This study was financially sponsored by the National Natural Science Foundation of China (grant No. 42005112, 42075144), the Open Funding of Zhejiang Key Laboratory of Ecological and Environmental Big Data (No. EEBD-2022-06), the Shanghai International Science and Technology Cooperation Fund (No.19230742500). This work is supported by Shanghai Technical Service Center of Science and Engineering Computing, Shanghai University.

References

Abalos, D., Jeffery, S., Sanz-Cobena, A., Guardia, G., and Vallejo, A.: Meta-analysis of the effect of urease and nitrification inhibitors on crop productivity and nitrogen use efficiency, Agriculture, Ecosystems & Environment, 189, 136-144, 2014.

Almaraz, M., Bai, E., Wang, C., Trousdell, J., Conley, S., Faloona, I., and Houlton, B. Z.: Agriculture is a major source of NO x pollution in California, Science advances, 4, eaao3477, 2018.

Cakaj, A., Qorri, E., Coulibaly, F., De Marco, A., Agathokleous, E., Leca, S., and Sicard, P.: Assessing surface ozone risk to human health and forests over time in Poland, Atmospheric Environment, 119926, 2023.

Chang, J., Brost, R., Isaksen, I., Madronich, S., Middleton, P., Stockwell, W., and Walcek, C.: A three‐dimensional Eulerian acid deposition model: Physical concepts and formulation, Journal of Geophysical Research: Atmospheres, 92, 14681-14700, 1987.

Chen, B., Wang, Y., Huang, J., Zhao, L., Chen, R., Song, Z., and Hu, J.: Estimation of near-surface ozone concentration and analysis of main weather situation in China based on machine learning model and Himawari-8 TOAR data, Science of The Total Environment, 864, 160928, 2023.

Chen, W., Guenther, A. B., Jia, S., Mao, J., Yan, F., Wang, X., and Shao, M.: Synergistic effects of biogenic volatile organic compounds and soil nitric oxide emissions on summertime ozone formation in China, Science of The Total Environment, 828, 154218, 2022.

Clappier, A., Belis, C. A., Pernigotti, D., and Thunis, P.: Source apportionment and sensitivity analysis: two methodologies with two different purposes, Geoscientific Model Development, 10, 4245-4256, 2017.

Diao, B., Ding, L., Su, P., and Cheng, J.: The spatial-temporal characteristics and influential factors of NOx emissions in China: A spatial econometric analysis, International journal of environmental research and Public Health, 15, 1405, 2018.

Ding, D., Xing, J., Wang, S., Dong, Z., Zhang, F., Liu, S., and Hao, J.: Optimization of a NO x and VOC cooperative control strategy based on clean air benefits, Environmental Science & Technology, 56, 739-749, 2021.

Ding, L., Liu, C., Chen, K., Huang, Y., and Diao, B.: Atmospheric pollution reduction effect and regional predicament: An empirical analysis based on the Chinese provincial NOx emissions, Journal of environmental management, 196, 178-187, 2017.

Drury, C. F., Reynolds, W. D., Yang, X., McLaughlin, N. B., Calder, W., and Phillips, L. A.: Diverse rotations impact microbial processes, seasonality and overall nitrous oxide emissions from soils, Soil Science Society of America Journal, 85, 1448-1464, 2021.

Du, L., Zhao, H., Tang, H., Jiang, P., and Ma, W.: Analysis of the synergistic effects of air pollutant emission reduction and carbon emissions at coal‐fired power plants in China, Environmental Progress & Sustainable Energy, 40, e13630, 2021.

Dunker, A. M., Koo, B., and Yarwood, G.: Source apportionment of the anthropogenic increment to ozone, formaldehyde, and nitrogen dioxide by the path-integral method in a 3D model, Environmental science & technology, 49, 6751-6759, 2015.

The volatile organic compound management attack program in 2020 (in Chinese): (available at:www.mee.gov.cn/xxgk2018/xxgk/xxgk03/202006/t20200624_785827.html), last

Feng, Z., De Marco, A., Anav, A., Gualtieri, M., Sicard, P., Tian, H., Fornasier, F., Tao, F., Guo, A., and Paoletti, E.: Economic losses due to ozone impacts on human health, forest productivity and crop yield across China, Environment international, 131, 104966, 2019.

Galbally, I. E., Kirstine, W. V., Meyer, C., and Wang, Y. P.: Soil–atmosphere trace gas exchange in semiarid and arid zones, Journal of Environmental Quality, 37, 599-607, 2008.

Guo, L., Chen, J., Luo, D., Liu, S., Lee, H. J., Motallebi, N., Fong, A., Deng, J., Rasool, Q. Z., and Avise, J. C.: Assessment of nitrogen oxide emissions and San Joaquin Valley PM2. 5 impacts from soils in California, Journal of Geophysical Research: Atmospheres, 125, e2020JD033304, 2020.

Heffer, P. and Prud'homme, M.: Global nitrogen fertilizer demand and supply: Trend, current level and outlook, International Nitrogen Initiative Conference. Melbourne, Australia,

Huang, K., Su, C., Liu, D., Duan, Y., Kang, R., Yu, H., Liu, Y., Li, X., Gurmesa, G. A., and Quan, Z.: A strong temperature dependence of soil nitric oxide emission from a temperate forest in Northeast China, Agricultural and Forest Meteorology, 323, 109035, 2022a.

Huang, L., Kimura, Y., and Allen, D. T.: Assessing the impact of episodic flare emissions on ozone formation in the Houston-Galveston-Brazoria area of Texas, Science of The Total Environment, 828, 154276, 2022b.

Huang, L., Wang, Q., Wang, Y., Emery, C., Zhu, A., Zhu, Y., Yin, S., Yarwood, G., Zhang, K., and Li, L.: Simulation of secondary organic aerosol over the Yangtze River Delta region: The impacts from the emissions of intermediate volatility organic compounds and the SOA modeling framework, Atmospheric Environment, 246, 118079, 2021.

Huber, D. E., Steiner, A. L., and Kort, E. A.: Sensitivity of Modeled Soil NOx Emissions to Soil Moisture, Journal of Geophysical Research: Atmospheres, 128, e2022JD037611, 2023.

Hudman, R. C., Moore, N. E., Mebust, A. K., Martin, R. V., Russell, A. R., Valin, L. C., and Cohen, R. C.: Steps towards a mechanistic model of global soil nitric oxide emissions: implementation and space based-constraints, Atmospheric Chemistry and Physics, 12, 7779-7795, 10.5194/acp-12-7779-2012, 2012.

Jiang, Y., Wang, S., Xing, J., Zhao, B., Li, S., Chang, X., Zhang, S., and Dong, Z.: Ambient fine particulate matter and ozone pollution in China: synergy in anthropogenic emissions and atmospheric processes, Environmental Research Letters, 17, 123001, 2022.

Koo, B., Wilson, G. M., Morris, R. E., Dunker, A. M., and Yarwood, G.: Comparison of source apportionment and sensitivity analysis in a particulate matter air quality model, Environmental science & technology, 43, 6669-6675, 2009.

Lin, Y., Jiang, F., Zhao, J., Zhu, G., He, X., Ma, X., Li, S., Sabel, C. E., and Wang, H.: Impacts of O3 on premature mortality and crop yield loss across China, Atmospheric Environment, 194, 41-47, 2018.

Liu, H. Z., Qingqing Liu: Distribution of Fertilizer Application and Its Environmental Risk in Different Provinces of China, Chemical Management, 174-174, 2016.

Liu, P., Song, H., Wang, T., Wang, F., Li, X., Miao, C., and Zhao, H.: Effects of meteorological conditions and anthropogenic precursors on ground-level ozone concentrations in Chinese cities, Environmental Pollution, 262, 114366, 2020.

Liu, X., Zhang, Y., Han, W., Tang, A., Shen, J., Cui, Z., Vitousek, P., Erisman, J. W., Goulding, K., and Christie, P.: Enhanced nitrogen deposition over China, Nature, 494, 459-462, 2013.

Lü, C. and Tian, H.: Spatial and temporal patterns of nitrogen deposition in China: synthesis of observational data, Journal of Geophysical Research: Atmospheres, 112, 2007.

Lu, X., Zhang, L., Wang, X., Gao, M., Li, K., Zhang, Y., Yue, X., and Zhang, Y.: Rapid increases in warm-season surface ozone and resulting health impact in China since 2013, Environmental Science & Technology Letters, 7, 240-247, 2020.

Lu, X., Ye, X., Zhou, M., Zhao, Y., Weng, H., Kong, H., Li, K., Gao, M., Zheng, B., and Lin, J.: The underappreciated role of agricultural soil nitrogen oxide emissions in ozone pollution regulation in North China, Nature communications, 12, 5021, 2021.

Maji, K. J.: Substantial changes in PM2. 5 pollution and corresponding premature deaths across China during 2015–2019: A model prospective, Science of the Total Environment, 729, 138838, 2020.

Malley, C. S., Henze, D. K., Kuylenstierna, J. C., Vallack, H. W., Davila, Y., Anenberg, S. C., Turner, M. C., and Ashmore, M. R.: Updated global estimates of respiratory mortality in adults ≥ 30 years of age attributable to long-term ozone exposure, Environmental health perspectives, 125, 087021, 2017.

Mao, J., Wang, L., Lu, C., Liu, J., Li, M., Tang, G., Ji, D., Zhang, N., and Wang, Y.: Meteorological mechanism for a large-scale persistent severe ozone pollution event over eastern China in 2017, Journal of Environmental Sciences, 92, 187-199, 2020.

Montes, C. M., Demler, H. J., Li, S., Martin, D. G., and Ainsworth, E. A.: Approaches to investigate crop responses to ozone pollution: from O3‐FACE to satellite‐enabled modeling, The Plant Journal, 109, 432-446, 2022.

Mukherjee, A., Yadav, D. S., Agrawal, S. B., and Agrawal, M.: Ozone a persistent challenge to food security in India: current status and policy implications, Current Opinion in Environmental Science & Health, 19, 100220, 2021.

Oikawa, P., Ge, C., Wang, J., Eberwein, J., Liang, L., Allsman, L., Grantz, D., and Jenerette, G.: Unusually high soil nitrogen oxide emissions influence air quality in a high-temperature agricultural region, Nature communications, 6, 8753, 2015.

Park, J., Shin, M., Lee, J., and Lee, J.: Estimating the effectiveness of vehicle emission regulations for reducing NOx from light-duty vehicles in Korea using on-road measurements, Science of The Total Environment, 767, 144250, 2021.

Potter, P., Ramankutty, N., Bennett, E. M., and Donner, S. D.: Characterizing the spatial patterns of global fertilizer application and manure production, Earth interactions, 14, 1-22, 2010.

Ramboll: User's Guide: Comprehensive Air quality Model with extensions, Version 7.1., 2021.

Rasool, Q. Z., Zhang, R., Lash, B., Cohan, D. S., Cooter, E. J., Bash, J. O., and Lamsal, L. N.: Enhanced representation of soil NO emissions in the Community Multiscale Air Quality (CMAQ) model version 5.0. 2, Geoscientific Model Development, 9, 3177-3197, 2016.

Romer, P. S., Duffey, K. C., Wooldridge, P. J., Edgerton, E., Baumann, K., Feiner, P. A., Miller, D. O., Brune, W. H., Koss, A. R., and De Gouw, J. A.: Effects of temperature-dependent NO x emissions on continental ozone production, Atmospheric Chemistry and Physics, 18, 2601-2614, 2018.

Sha, T., Ma, X., Zhang, H., Janechek, N., Wang, Y., Wang, Y., Castro García, L., Jenerette, G. D., and Wang, J.: Impacts of Soil NO x Emission on O3 Air Quality in Rural California, Environmental science & technology, 55, 7113-7122, 2021.

Shen, L., Liu, J., Zhao, T., Xu, X., Han, H., Wang, H., and Shu, Z.: Atmospheric transport drives regional interactions of ozone pollution in China, Science of The Total Environment, 830, 154634, 2022.

Shen, Y., Xiao, Z., Wang, Y., Xiao, W., Yao, L., and Zhou, C.: Impacts of agricultural soil NOx emissions on O3 over Mainland China, Journal of Geophysical Research: Atmospheres, e2022JD037986, 2023.

Skiba, U., Medinets, S., Cardenas, L. M., Carnell, E. J., Hutchings, N., and Amon, B.: Assessing the contribution of soil NO x emissions to European atmospheric pollution, Environmental Research Letters, 16, 025009, 2021.

State Council: The 14th Five-Year Plan for National Economic and Social Development of the People's Republic of China and the Outline of Long-Term Objectives for 2035, 2021.

Sun, W., Shao, M., Granier, C., Liu, Y., Ye, C., and Zheng, J.: Long‐term trends of Anthropogenic SO2, NOx, CO, and NMVOCs emissions in China, Earth's Future, 6, 1112-1133, 2018.

Sun, Y., Yin, H., Lu, X., Notholt, J., Palm, M., Liu, C., Tian, Y., and Zheng, B.: The drivers and health risks of unexpected surface ozone enhancements over the Sichuan Basin, China, in 2020, Atmospheric Chemistry and Physics, 21, 18589-18608, 2021.

Thunis, P., Clappier, A., Tarrasón, L., Cuvelier, C., Monteiro, A., Pisoni, E., Wesseling, J., Belis, C., Pirovano, G., and Janssen, S.: Source apportionment to support air quality planning: Strengths and weaknesses of existing approaches, Environment International, 130, 104825, 2019.

Vinken, G., Boersma, K., Maasakkers, J., Adon, M., and Martin, R.: Worldwide biogenic soil NO x emissions inferred from OMI NO 2 observations, Atmospheric Chemistry and Physics, 14, 10363-10381, 2014.

Wang, J., Wang, D., Ge, B., Lin, W., Ji, D., Pan, X., Li, J., and Wang, Z.: Increase in daytime ozone exposure due to nighttime accumulation in a typical city in eastern China during 2014–2020, Atmospheric Pollution Research, 13, 101387, 2022a.

Wang, P., Wang, T., and Ying, Q.: Regional source apportionment of summertime ozone and its precursors in the megacities of Beijing and Shanghai using a source-oriented chemical transport model, Atmospheric Environment, 224, 117337, 2020.

Wang, Q. g., Han, Z., Wang, T., and Zhang, R.: Impacts of biogenic emissions of VOC and NOx on tropospheric ozone during summertime in eastern China, Science of the total environment, 395, 41-49, 2008.

Wang, R., Bei, N., Wu, J., Li, X., Liu, S., Yu, J., Jiang, Q., Tie, X., and Li, G.: Cropland nitrogen dioxide emissions and effects on the ozone pollution in the North China plain, Environ Pollut, 294, 118617, 10.1016/j.envpol.2021.118617, 2022b.

Wang, Y., Ge, C., Garcia, L. C., Jenerette, G. D., Oikawa, P. Y., and Wang, J.: Improved modelling of soil NO x emissions in a high temperature agricultural region: role of background emissions on NO2 trend over the US, Environmental research letters, 16, 084061, 2021.

Xiao, Q., Geng, G., Liang, F., Wang, X., Lv, Z., Lei, Y., Huang, X., Zhang, Q., Liu, Y., and He, K.: Changes in spatial patterns of PM2. 5 pollution in China 2000–2018: Impact of clean air policies, Environment international, 141, 105776, 2020.

Xue, C., Ye, C., Liu, P., Zhang, C., Su, H., Bao, F., Cheng, Y., Catoire, V., Ma, Z., and Zhao, X.: Strong HONO Emissions from Fertilized Soil in the North China Plain 4 Driven by Nitrification and Water Evaporation, 2022.

Yan, X., Ohara, T., and Akimoto, H.: Statistical modeling of global soil NOx emissions, Global Biogeochemical Cycles, 19, 2005.

Yang, X., Wu, K., Lu, Y., Wang, S., Qiao, Y., Zhang, X., Wang, Y., Wang, H., Liu, Z., and Liu, Y.: Origin of regional springtime ozone episodes in the Sichuan Basin, China: role of synoptic forcing and regional transport, Environmental Pollution, 278, 116845, 2021.

Yarwood, G., Morris, R., Yocke, M., Hogo, H., and Chico, T.: Development of a methodology for source apportionment of ozone concentration estimates from a photochemical grid model, AIR & WASTE MANAGEMENT ASSOCIATION, PITTSBURGH, PA 15222(USA).[np]. 1996.

Yarwood, G., Jung, J., Whitten, G. Z., Heo, G., Mellberg, J., and Estes, M.: Updates to the Carbon Bond mechanism for version 6 (CB6), 9th Annual CMAS Conference, Chapel Hill, NC, 11-13,

Yienger, J. and Levy, H.: Empirical model of global soil‐biogenic NO$_x$ emissions, Journal of Geophysical Research: Atmospheres, 100, 11447-11464, 1995.

Yin, H., Lu, X., Sun, Y., Li, K., Gao, M., Zheng, B., and Liu, C.: Unprecedented decline in summertime surface ozone over eastern China in 2020 comparably attributable to anthropogenic emission reductions and meteorology, Environmental Research Letters, 16, 124069, 2021.

Zhai, S., Jacob, D. J., Wang, X., Shen, L., Li, K., Zhang, Y., Gui, K., Zhao, T., and Liao, H.: Fine particulate matter (PM2.5) trends in China, 2013–2018: separating contributions from anthropogenic emissions and meteorology, Atmospheric Chemistry and Physics, 19, 11031-11041, 2019.

Zheng, B., Zhang, Q., Geng, G., Chen, C., Shi, Q., Cui, M., Lei, Y., and He, K.: Changes in China's anthropogenic emissions and air quality during the COVID-19 pandemic in 2020, Earth System Science Data, 13, 2895-2907, 2021.